

This is the accepted manuscript made available via CHORUS. The article has been published as:

## Unusual field dependence of spin fluctuations on different timescales in $\text{Tb}_{\{2\}}\text{Ti}_{\{2\}}\text{O}_{\{7\}}$

P. J. Baker, M. J. Matthews, S. R. Giblin, P. Schiffer, C. Baines, and D. Prabhakaran

Phys. Rev. B **86**, 094424 — Published 19 September 2012

DOI: [10.1103/PhysRevB.86.094424](https://doi.org/10.1103/PhysRevB.86.094424)

# Unusual field dependence of spin fluctuations on different timescales in $\text{Tb}_2\text{Ti}_2\text{O}_7$

P. J. Baker,<sup>1</sup> M. J. Matthews,<sup>2</sup> S. R. Giblin,<sup>1</sup> P. Schiffer,<sup>2</sup> C. Baines,<sup>3</sup> and D. Prabhakaran<sup>4</sup>

<sup>1</sup>*ISIS Facility, STFC Rutherford Appleton Laboratory, Didcot OX11 0QX, United Kingdom*

<sup>2</sup>*Department of Physics and Materials Research Institute,*

*Pennsylvania State University, University Park, Pennsylvania 16802, USA*

<sup>3</sup>*Laboratory for Muon-Spin Spectroscopy, Paul Scherrer Institute, Villigen CH-5232, Switzerland*

<sup>4</sup>*Oxford University Department of Physics, Clarendon Laboratory,  
Parks Road, Oxford OX1 3PU, United Kingdom*

(Dated: September 4, 2012)

We have investigated the spin dynamics of  $\text{Tb}_2\text{Ti}_2\text{O}_7$  as a function of magnetic field applied along the [111] axis using ac susceptibility and muon-spin relaxation measurements. We find a significant increase in the imaginary part of the magnetic susceptibility at low fields at our lowest investigated temperature and an increased muon-spin relaxation rate in the same field range persisting to higher temperature. Comparing the data from the two techniques we identify three field regions where the dynamic properties of  $\text{Tb}_2\text{Ti}_2\text{O}_7$  appear to be evolving in different ways with crossovers between the regions at  $B_1 = 15$  and  $B_2 \sim 60$  mT.

PACS numbers: 76.75.+i, 75.40.Gb, 75.50.Ee

Frustration in magnetism can arise because of geometrically-induced competition between interactions, preventing local magnetic moments from ordering down to temperatures well below the energy scale of those interactions. If magnetic fluctuations persist to the lowest experimentally accessible temperatures without the development of a static order parameter, the low temperature magnetic state can be described as a cooperative paramagnet or spin liquid. Such systems provide considerable opportunities for experimental tests of theoretical approaches to exotic collective phenomena.<sup>1</sup> In this context the pyrochlore magnet  $\text{Tb}_2\text{Ti}_2\text{O}_7$  has proved an intriguing conundrum since no magnetic ordering is observed down to the lowest measured temperature,  $\sim 15$  mK, far below the Curie-Weiss temperature,  $\Theta_{\text{CW}} = -19$  K,<sup>2</sup> and on this basis it has been identified as a potential three-dimensional spin liquid.<sup>1-7</sup>

Two alternate theoretical proposals have recently been suggested to account for the lack of observed magnetic ordering in  $\text{Tb}_2\text{Ti}_2\text{O}_7$ : the first considers a Jahn-Teller-like distortion and a two-singlet system coupled by exchange,<sup>8</sup> whilst the second has proposed that quantum fluctuations of the  $\text{Tb}^{3+}$  magnetic moments can renormalize the low-energy effective Hamiltonian of the system from an unfrustrated  $\langle 111 \rangle$  Ising antiferromagnet to a frustrated  $\langle 111 \rangle$  Ising ferromagnet.<sup>9</sup> The quantum fluctuation theory is of interest as it suggests  $\text{Tb}_2\text{Ti}_2\text{O}_7$  is a quantum analog of the classical spin ice systems  $\text{Dy}_2\text{Ti}_2\text{O}_7$  and  $\text{Ho}_2\text{Ti}_2\text{O}_7$ ,<sup>10,11</sup> a quantum spin ice state. Indeed the same degenerate ground state is present in both water ice and spin ice, and theoretical work has demonstrated that quantum mechanical tunnelling between different spin- or charge-ice configurations can lead to a resolution of this issue.<sup>12</sup> The magnetic Coulomb phase has been shown to exist in classical dipolar spin ice as a magnetic analogy of electrostatics<sup>13</sup> and quantum spin ice should display a magnetic analog of quantum electrodynamics.<sup>14</sup> Experimental evidence for quan-

tum spin liquid states that are the quantum mechanical analogs of spin ice have recently been found in the pyrochlore materials  $\text{Yb}_2\text{Ti}_2\text{O}_7$ <sup>15,16</sup> and in  $\text{Pr}_2\text{Sn}_2\text{O}_7$ ,<sup>17,18</sup> whereas for  $\text{Tb}_2\text{Ti}_2\text{O}_7$  there have only been theoretical predictions of such phenomena.<sup>9,23</sup>

Recent experimental work has attempted to distinguish between the two theoretical predictions for  $\text{Tb}_2\text{Ti}_2\text{O}_7$  with evidence presented for<sup>19,20</sup> and against<sup>21</sup> the proposed singlet ground state.<sup>8</sup> In addition other work has suggested the existence of quantum spin fluctuations at low temperatures.<sup>22</sup> Another way to distinguish between the theoretical models for the origin of the low temperature fluctuations is to explicitly test one of their predictions. Importantly, when the quantum spin ice model<sup>9</sup> is applied to  $\text{Tb}_2\text{Ti}_2\text{O}_7$  it is predicted that for small fields applied along the [111] crystal axis a similar evolution between magnetic states to that in the thoroughly investigated partial magnetization plateaux<sup>24-27</sup> in  $\text{Dy}_2\text{Ti}_2\text{O}_7$  and  $\text{Ho}_2\text{Ti}_2\text{O}_7$  will be observed, albeit with a far smaller characteristic field scale,  $\lesssim 0.1$  T. At the lowest temperatures,  $\ll 0.1$  K, a partial magnetization plateau should be evident<sup>23</sup> in this field region. While the underlying magnetic states should persist to slightly higher temperatures the small bandwidth of the energy levels results in the predicted plateau being smeared by around 0.1 K. The energy scales for  $\text{Tb}_2\text{Ti}_2\text{O}_7$  are significantly reduced due to the effect of the quantum fluctuations. If the effective exchange constant is above the critical value then the system will instead show all-in-all-out magnetism. Since we completed our experimental work three studies have searched for the predicted plateau using bulk magnetic measurements without finding exact agreement with the theoretical predictions.<sup>28-30</sup> It is known that perturbations drive  $\text{Tb}_2\text{Ti}_2\text{O}_7$  into a magnetically ordered phase, this has been demonstrated by applying magnetic fields<sup>31-35</sup> and pressure<sup>36</sup>. Structural fluctuations are also observed in zero magnetic field,<sup>37</sup> with phase transitions observed in fields larger

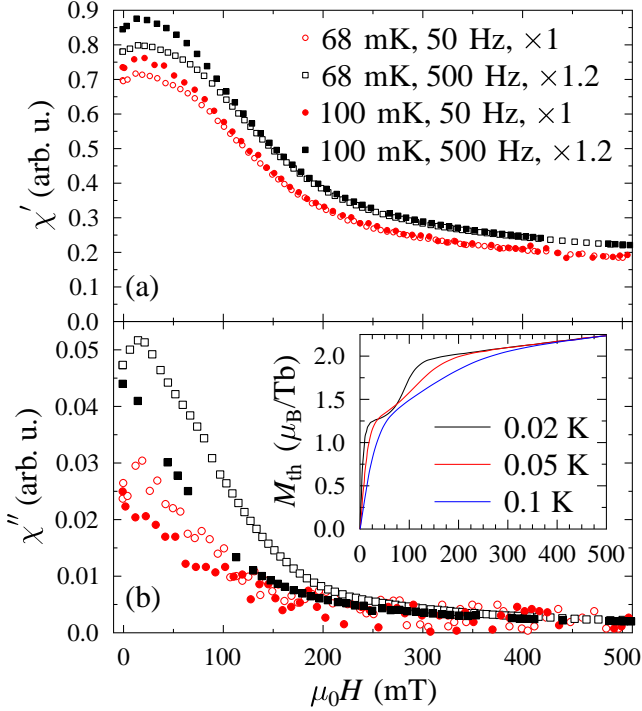


FIG. 1: (Color online) ac susceptibility data with the field applied  $\parallel$  [111]: (a) Real part  $\chi'$ , (b) Imaginary part  $\chi''$ . The data are offset for clarity. (Inset) Theoretical magnetization curves predicted by the quantum spin ice model of Ref. 23 for  $J = 0.167$  K.

than 25 T<sup>38</sup> and the presence of a tetragonal lattice distortion is also seen.<sup>39</sup> However, most work has focussed on magnetic fields far larger than those relevant to finding the predicted plateau.

Here we report an experimental investigation of the spin dynamics of  $Tb_2Ti_2O_7$  using ac susceptibility and muon spin relaxation ( $\mu$ SR) experiments with a magnetic field applied along the [111] axis in both cases. The former technique provides information on the quasistatic bulk magnetism whereas the latter probes the local dynamic magnetic correlations within a time window of  $10^{-12} - 10^{-6}$  s. We are able to identify three field regions where the dynamic behavior behaves differently as the field applied along the [111] axis is changed.

All our experiments were performed on single crystals of  $Tb_2Ti_2O_7$  grown via the floating zone method. Initial characterization of the sample with a SQUID magnetometer revealed a Curie Weiss constant of  $-17$  K, in close agreement with the published literature,<sup>2</sup> and all crystals were aligned along the [111] axis using the back scattering x-ray Laue technique. The ac susceptibility measurements were performed using a custom made coil set, thermally anchored to the mixing chamber of an Oxford Instruments dilution refrigerator through immersion in liquid  $^4He$ . For our  $\mu$ SR measurements<sup>40</sup> we performed experiments at the pulsed ISIS muon source (MuSR spectrometer) and the continuous PSI source [Low Temper-

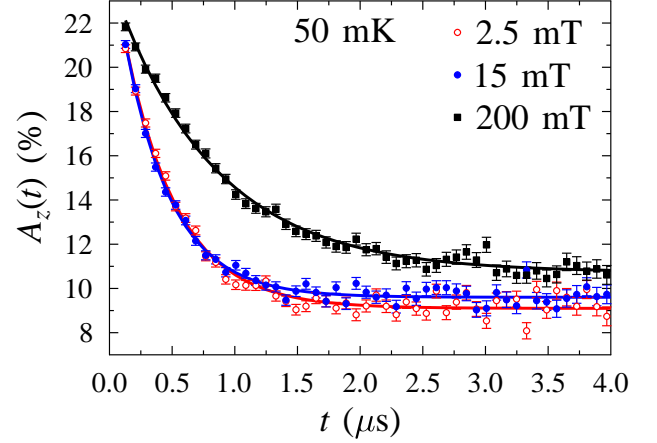


FIG. 2: (Color online) Longitudinal field  $\mu$ SR data at 50 mK as a function of applied field along the [111] axis. The solid lines are the fits to the data described in the text.

ature Fridge (LTF) spectrometer], ensuring both long and short time resolution. The magnetic field was parallel to the initial muon spin polarization [longitudinal field (LF)] in the ISIS measurements ( $0.05 < T < 10$  K) and with the initial muon spin polarization partially rotated [LF and transverse field (TF)] for measurements ( $0.025 < T < 0.9$  K) using the LTF spectrometer. In both cases a crystal mosaic was used allowing a total coverage of 2.5 cm<sup>2</sup> at ISIS and 1.0 cm<sup>2</sup> at PSI and attached to a silver backing plate using a thin layer of GE varnish. The silver plate gives a background signal that can easily be identified and subtracted from the asymmetry data. The measured parameter is the time-dependent muon decay asymmetry,  $A(t)$ , recorded in positron detectors on opposite sides of the sample, which provides a measure of the spin polarization of the muon ensemble as a function of time.

The ac susceptibility data are shown in Figure 1 (a) for the real part  $\chi'$  and (b) for the imaginary part  $\chi''$ . The data recorded at 100 and 125 mK are equivalent within error (125 mK data not shown) but there is a clear separation between these data and those recorded at 68 mK in both components of the susceptibility. In  $\chi'$  the separation is clear below  $\sim 200$  mT and grows towards zero field. Other measurements of the ac susceptibility have indicated a bifurcation with applied field at low temperature and a frequency dependence consistent with our results.<sup>7,28,30,41</sup> Our data are also in reasonable agreement with other measurements of  $dM/dH$  by Legl *et al.*<sup>29</sup> and  $\chi'$  by Yin *et al.*<sup>30</sup> at these temperatures, though the latter study found a subsequent change in the field dependence of  $\chi'$  cooling to 16 mK, accompanied by exceptionally long magnetic relaxation times. The temperature dependence is more pronounced in  $\chi''$ , where at 68 mK the susceptibility rises to a peak at 15 mT but at  $\geq 100$  mK it falls monotonically. The difference between  $\chi''$  at these two temperatures is up to a factor of two and their val-

ues are distinct up to  $\sim 100 - 300$  mT depending on the measurement frequency. We have plotted the theoretical magnetization curves<sup>23</sup> in the inset to Fig. 1 and return to comparing these data with the theoretical predictions below, since our measurement temperature is too high to test the predicted partial magnetization plateau directly.

As a local probe of spin fluctuations  $\mu$ SR is an ideal tool to look for systematic changes in  $\text{Tb}_2\text{Ti}_2\text{O}_7$ . The  $\mu$ SR data recorded in longitudinal field are shown in Fig. 2 and can all be described by an exponential relaxation:

$$A_z(t) = A_{\text{rlx}}e^{-\lambda t} + A_{\text{bg}}, \quad (1)$$

where  $\lambda$  is the muon spin relaxation rate. The values of  $A_{\text{rlx}}$  and  $A_{\text{bg}}$  vary according to the cryostat used (0.025 K LTF instrument, 0.05 - 0.725 K Oxford Instruments Kelvinox, 1.5 and 2 K Oxford Instruments Variox, and 5 and 10 K closed-cycle refrigerator) due to differing beam spot sizes, scattering in cryostat windows, and the momentum degradation of muons passing through different thickness of cryostat walls before hitting the detectors.  $A_{\text{rlx}}$  varies significantly with field below 0.725 K but is close to field independent at higher temperature [Fig. 2 (b)]. The field dependence of  $A_{\text{bg}}$  shown in Fig. 2 (c), and decoupling in small longitudinal applied field of the weak background relaxation, are both consistent with the expected behaviour of the silver sample holder. The behavior of the fitted parameters is consistent between the measurements at pulsed and continuous muon sources. Equation 1 describes the data over the entire field range demonstrating that the fluctuations remain dynamic on the timescale probed by muons, and the results we report are quantitatively consistent with those in Ref. 20 at the same fields and temperatures, although the fit of our data is not improved by fitting a stretched exponential over the field range we have studied.<sup>43</sup>

For the  $T \leq 2$  K longitudinal field data, three regions can be identified in the field dependent relaxation rates shown in Fig. 3 (a). At small fields up to  $B_1 = 15$  mT,  $\lambda$  increases to a peak, then falls steeply to a kink at  $B_2 \sim 60$  mT, followed by a more gradual fall between 60 and 250 mT. The data recorded for  $T \leq 0.725$  K lie over one another so only the 50 mK data are plotted for clarity. The low-temperature, low-field increase in  $\lambda$  up to  $B_1$  resembles the behavior seen<sup>44</sup> in  $\text{Tb}_2\text{Sn}_2\text{O}_7$  where the increase has a gradient of 0.11 MHz/mT although in our data the increase is rather smaller: 0.035(5) MHz/mT. From other measurements it is clear that the ground states are distinct, but such an increase could result from a field-induced increase in the density of low energy excitations as suggested<sup>44</sup> for  $\text{Tb}_2\text{Sn}_2\text{O}_7$  or, more prosaically, a steep change in the local magnetization at low fields that increases the distribution of local fields probed by the muon. For comparison, we plot the trend  $\lambda(B_{\text{LF}}) \propto B^{-1}$  previously found for polycrystalline data at 100 mK<sup>47</sup> as a solid line in Fig. 3 (a). This is similar to the behaviour seen in our data above  $\sim 70$  mT, showing

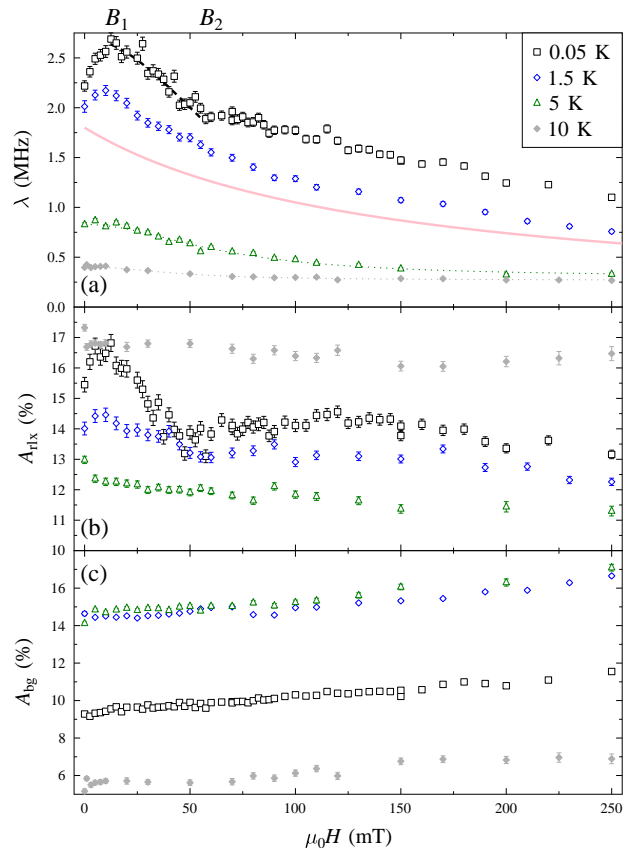


FIG. 3: (Color online) (a) Relaxation rate  $\lambda$  measured as a function of longitudinal magnetic field applied along the [111] axis. The solid line represents the trend for a polycrystalline sample at 0.1 K reported in Ref. 47. The dashed and dotted lines represent fits described in the text. (b) and (c) The relaxing asymmetry and background asymmetry.

that the peak and kink observed below 2 K are due to the orientation of the sample.

The magnetic fluctuations in  $\text{Tb}_2\text{Ti}_2\text{O}_7$  have previously been shown to be fast compared with the range of timescales probed by muons,<sup>3,46-48</sup> that is to say that the system is paramagnetic on the muon timescale. As a starting point in describing the field-dependent exponential relaxation rate  $\lambda$ , we relate it to the distribution width of magnetic fields at the muon stopping site  $\Delta$ , the fluctuation time  $\tau$ , and the applied longitudinal field  $B_{\text{LF}}$  by the sum of Redfield's equation,<sup>49</sup> which is generally appropriate for exponential muon spin relaxation, and a field-independent relaxation rate  $\lambda_0$ ,

$$\lambda = \frac{2\gamma_\mu^2 \Delta^2 \tau}{1 + \gamma_\mu^2 B_{\text{LF}}^2 \tau^2} + \lambda_0. \quad (2)$$

Our data appear to tend to a field-independent value  $\lambda_0$  above 0.25 T, which is consistent with the behavior seen in that field range in Ref. 46 and, while adding  $\lambda_0$  alters the values of  $\Delta$  and  $\tau$  extracted from the data, this equation allows us to describe the whole measured field

range consistently for  $T \geq 5$  K. For  $T \leq 2$  K this function cannot describe the data over the whole field range with constant values of  $\Delta$  and  $\tau$ . This suggests that either  $\Delta$  and  $\tau$  depend on the applied field or an alternative model is needed for the muon spin relaxation mechanism.

The effectiveness of equation 2 is contingent on their being a single correlation time relevant in the field range under investigation. A more complicated distribution of correlation times would lead to a more complicated field dependence, although the relaxation rate would not be expected to increase as a function of field, as is observed in our low-temperature data up to  $B_1$ . This problem was noted previously<sup>44</sup> for the increase in  $\lambda$  at small fields observed in  $\text{Tb}_2\text{Sn}_2\text{O}_7$ . Such an increase, within the Redfield picture, requires  $\Delta$  and/or  $\tau$  to vary with field, or the presence of other relaxation mechanisms. Above the peak,  $B_1$ , a distribution of fields and/or timescales, which commonly occurs in frustrated magnets, might give rise to the two stages apparent in the field dependence either side of  $B_2$ . A broad distribution of fields or timescales generally gives rise to a stretched exponential relaxation  $\exp[-(\lambda t)^\beta]$  with  $1/3 < \beta < 1$ , with  $\beta$  decreasing as the distributions broaden. This is not consistent with our data for which  $\beta = 1$ , nor other published data<sup>20</sup> where  $\beta$  was slightly larger than 1. Therefore our results constrain the widths of the field and correlation time distributions to be relatively narrow, and if this is to apply over the whole measured field range then a more complicated relaxation mechanism than is captured in eq. 2 must depolarize the muon spin.

Another potential relaxation mechanism appropriate to fluctuating localized magnetic moments<sup>45</sup> relates the muon relaxation rate  $\lambda$  to the imaginary part of the dynamic susceptibility  $\chi''(\mathbf{q}, \omega)$  as:  $\lambda \propto \int_{\mathbf{q}} A(\mathbf{q}) \chi''(\mathbf{q}, \omega)$ , where  $A(\mathbf{q})$  is the coupling between the muon spin and the spins of the sample. The relevant frequency in these longitudinal field measurements varies with the applied field as  $\omega = \gamma_\mu B$ . We know  $\chi''(\omega \rightarrow 0)$  from our ac susceptibility measurements shown in Fig. 1(b) and so begin our comparison with the observed  $\lambda$  values there. In the 68 mK data  $\chi''$  rises to a peak at  $B_1$  coincident with that in  $\lambda$  for  $T \leq 2$  K, whereas at 100 mK  $\chi''$  falls monotonically with field, as  $\lambda$  does for  $T \geq 5$  K. There are therefore similarities in the field dependences, but the temperature scale is quite distinct. The relevant frequencies for the two probes are around kHz for ac susceptibility and GHz for  $\mu\text{SR}$  and so a difference in  $\chi''(T, \omega, B)$  at these disparate frequencies is required. A simple possibility is thermal fluctuations of the low-temperature state leaving the frequency range of ac susceptibility by around 100 mK but remaining within the  $\mu\text{SR}$  frequency range to around 2 K. Alternatively  $\chi''$  may depend strongly on  $\omega$  for the range of muon Larmor frequencies corresponding to  $0 < B < 60$  mT.

The Redfield model would also break down if the field distribution changed within the region investigated. Systems with metamagnetic transitions would lead to such a breakdown and if the other conditions for ap-

plying the Redfield equation are satisfied then  $\lambda$  could follow the simple phenomenological form of equation 2 between transitions if the arrangement of spins is consistent within the region. By way of example, equation 2 was found to apply in the partial magnetization plateau phase of  $\text{Ca}_3\text{Co}_2\text{O}_6$  where the magnetization plateau is known from a broad range of techniques.<sup>42</sup>

Using equation 2, we can test predictions for the field dependence of  $\Delta$  and  $\tau$ . The simplest assumption is that neither depends on field, which effectively describes both the 5 and 10 K data. Below 5 K this model does not work over the whole field range. However, it is effective between the peak ( $B_1$ ) and kink ( $B_2$ ) shown in Fig. 3, and also above  $B_2$  with different parameters. Fitting (with  $\lambda_0 = 0$ ) leads to  $\Delta = 12.0(2)$  mT and  $\tau = 12.8(6)$  ns at 50 mK between  $B_1$  and  $B_2$ , the fit for 50 mK being shown as the dashed line in Figure 3. Above  $B_2$ , the same fitting approach gives  $\Delta = 17.7(1)$  mT and  $\tau = 4(1)$  ns. Including the  $\lambda_0$  values estimated using the fits to the data above  $B_2$  ( $\lambda_0 \sim 0.5$  MHz) reduces the value of  $\Delta$  by around 15 % and increases  $\tau$  by around 10 %. Independent of this, the quality of the fits are poorer for the 1.5 and 2 K data, which is consistent with thermal fluctuations breaking up the low temperature state.

This phenomenological change of the field dependence of the relaxation can be clearly seen if the data is plotted as  $\lambda^{-1}$  vs  $B^2$ , since the Redfield equation is linear in these parameters. Fig. 4 shows the field dependence of the inverse relaxation rate as a function of temperature. It is clear that eq. 2 is valid over two distinct regions: from the peak  $B_1 = 15$  mT to the kink  $B_2 \sim 60$  mT and above the kink  $B_2$ .  $B_1$  also matches the peak seen in our measurements of  $\chi''$  but we do not see a sharply defined feature at  $B_2$  in the ac susceptibility or any features in  $\lambda$  in the field region where  $\chi'(H)$  flattens.

This leads to the question of what causes this non-monotonic field dependence of  $\lambda$ . It could come from complicated distribution of relaxation times, although this would suggest the raw data should take a stretched, rather than simple exponential form. We cannot exclude such a possibility but were unable to develop a simple model that could consistently describe both the field dependence above  $B_1$  and the observed form of the raw data. If we compare the field dependence of  $\lambda$  to that of  $\chi''$  then we see strong similarities in the features in  $\lambda$  below 2 K to those in  $\chi''$  at 68 mK, and in  $\lambda$  above 5 K and  $\chi''$  at 100 mK. The disparity between the temperatures where these features occur could follow simply from the effect of thermal fluctuations measured on the different timescales of the two probes. If the relaxation mechanism is relatively conventional and there is one (dominant) correlation time, as suggested by the simple exponential form of the raw data, then the features in the data may be associated with changes occurring in the magnetic correlations within the sample, as could separately follow from the similarities in the field dependences of  $\chi''$  and  $\lambda$ . We use eq. 2 to provide a starting point for interpreting the data. This would imply three regions in the

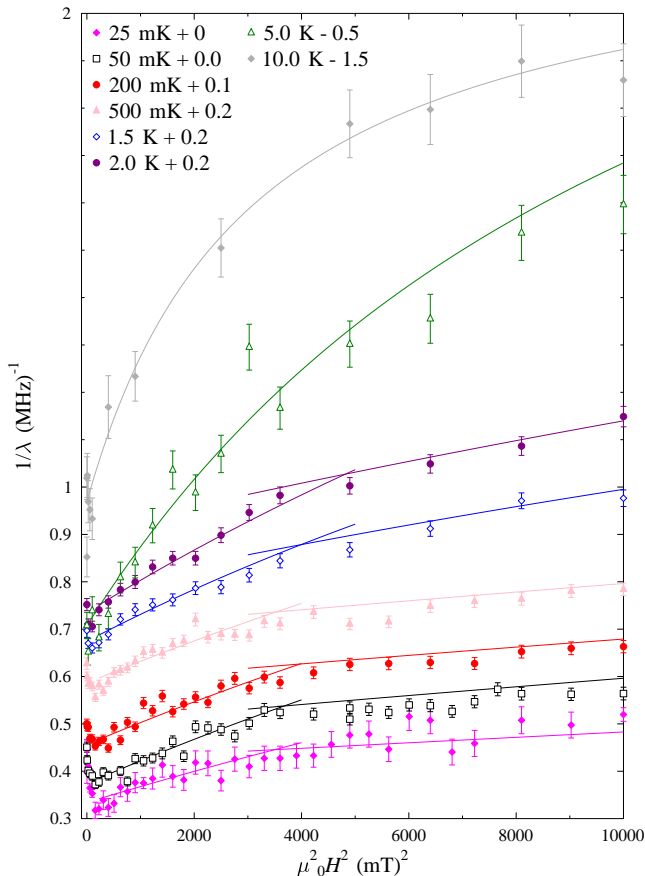


FIG. 4: (Color online) Field dependence of the inverse relaxation rate at different temperatures. The fitted lines are eq. 2 for different field ranges. The data are offset for clarity and the higher field fits extend to the maximum measured field.

field dependence: the first up to  $B_1$  where  $\Delta$  increases (or  $\tau$  decreases) with field sufficiently quickly for the numerator of eq. 2 to increase faster than the denominator, and then two regions where  $\Delta$  and  $\tau$  take separately constant values, or their field dependences counteract.

The only theoretical suggestion advanced for features in this field range comes from the quantum spin ice model proposed by Molavian and Gingras<sup>23</sup>, with crossovers between spin arrangements on individual tetrahedra occurring at  $B^* \approx 16$  mT and  $B_c \approx 82$  mT, depending on the effective exchange constant within the model. The energy scheme for these arrangements was argued to be relevant below a temperature of order 1 K, where the spin correlations have developed up to the size of a single tetrahedron,<sup>3,5-7</sup> but the associated partial magnetization plateau predicted in the same work would only be observed well below 0.1 K, perhaps even below 0.02 K, because of the small bandwidth of the lowest lying states.<sup>23</sup> This model has been tested down to 43 mK using bulk magnetization measurements and no evidence for a partial magnetization plateau was found.<sup>28,29</sup> Our measurements of  $\chi'$  and those of Yin *et al.*<sup>30</sup> are in reasonable

qualitative agreement with the  $dM/dH$  curves of Legl *et al.*<sup>29</sup> in this temperature range and Legl *et al.* argued that  $\text{Tb}_2\text{Ti}_2\text{O}_7$  has an all-in/all-out ground state at low temperature. The field-dependent properties of such a state do not give rise to any features in the range where features occur in the  $\mu\text{SR}$  or  $\chi''$  data. A very recent ac susceptibility study<sup>30</sup> found a further change in  $\chi'(B)$  between 50 and 16 mK and it may be necessary to extend the bulk magnetization measurements to a similarly low temperature to provide a firm conclusion on this matter. Other descriptions of  $\text{Tb}_2\text{Ti}_2\text{O}_7$  in terms of a Jahn-Teller distortion have not made predictions for its response to small [111] magnetic fields and it would be interesting to know whether any features could be predicted compatible with the recent results in this area. In general, models of  $\text{Tb}_2\text{Ti}_2\text{O}_7$  have not offered predictions for multiple timescales, nor for multiple field distributions, but the future development of more detailed models may offer another framework for describing our results.

In conclusion, we have presented low-temperature ac susceptibility and  $\mu\text{SR}$  data on  $\text{Tb}_2\text{Ti}_2\text{O}_7$  for fields applied along the [111] crystal axis. At low fields the  $\mu\text{SR}$  relaxation rate  $\lambda$  rises to a peak at  $B_1 = 15$  mT, after which it falls steeply to a kink around  $B_2 \sim 60$  mT and then more gradually to higher fields. This field dependence is not evident in polycrystalline samples and by making a simple assumption as to its origin we can estimate the timescale of fluctuations to be  $\tau \sim 10$  ns. The temperature dependence of these features is very weak below 0.725 K and then they disappear smoothly up to 5 K, similar to the saturation of  $\lambda$  below 1 K observed in previous measurements in constant magnetic fields.<sup>3,20</sup> Our measurements of  $\chi'$  below 100 mK do not show sharp features coincident with those in the  $\mu\text{SR}$  data, but  $\chi''$  shows a peak at  $B_1$  at 68 mK which has disappeared at 100 mK. These differences strongly suggest that the response of  $\text{Tb}_2\text{Ti}_2\text{O}_7$  depends on the lengthscale and timescale being probed. To develop a broader understanding of this field-dependent behavior, bridging the gap in timescales we report here with higher frequency ac susceptibility measurements at very low temperatures and neutron scattering measurements, since the fluctuations affecting the muon relaxation would be quasistatic on their timescale, would complete this picture and provide a further constraint on future theoretical models of  $\text{Tb}_2\text{Ti}_2\text{O}_7$ .

We thank Andrew Boothroyd for help with crystal preparation, Larry Linfitt and the ISIS cryogenics group for experimental assistance, Liang Yin, Francis Pratt, and Michel Gingras for helpful discussions, STFC (UK) for provision of beamtime, and NSF grant DMR-0701582 and DMR-1104122 for support of MJM and PS. Part of this work was done at the Swiss Muon Source, Paul Scherrer Institute, CH.

- <sup>1</sup> L. Balents, *Nature* **464**, 199 (2010).
- <sup>2</sup> J. S. Gardner, M. J. P. Gingras, and J. E. Greedan, *Rev. Mod. Phys.* **82**, 53 (2010).
- <sup>3</sup> J. S. Gardner, S. R. Dunsiger, B. D. Gaulin, M. J. P. Gingras, J. E. Greedan, R. F. Kiefl, M. D. Lumsden, W. A. MacFarlane, N. P. Raju, J. E. Sonier, I. Swainson, and Z. Tun, *Phys. Rev. Lett.* **82**, 1012 (1999).
- <sup>4</sup> M. J. P. Gingras, B. C. den Hertog, M. Faucher, J. S. Gardner, S. R. Dunsiger, L. J. Chang, B. D. Gaulin, N. P. Raju, and J. E. Greedan, *Phys. Rev. B* **62**, 6496 (2000).
- <sup>5</sup> J. S. Gardner, B. D. Gaulin, A. J. Berlinsky, P. Waldron, S. R. Dunsiger, N. P. Raju, and J. E. Greedan, *Phys. Rev. B* **64**, 224416 (2001).
- <sup>6</sup> Y. Yasui, M. Kanada, M. Ito, H. Harashina, M. Sato, H. Okumura, K. Kakurai, and H. Kadowaki, *J. Phys. Soc. Japan* **71**, 599 (2002).
- <sup>7</sup> J. S. Gardner, A. Keren, G. Ehlers, C. Stock, E. Segal, J. M. Roper, B. Fåk, M. B. Stone, P. R. Hammar, D. H. Reich, and B. D. Gaulin, *Phys. Rev. B* **68**, 180401(R) (2003).
- <sup>8</sup> P. Bonville, I. Mirebeau, A. Gukasov, S. Petit, and J. Robert, *Phys. Rev. B* **84**, 184409 (2011).
- <sup>9</sup> H. R. Molavian, M. J. P. Gingras, and B. Canals, *Phys. Rev. Lett.* **98**, 157204 (2007).
- <sup>10</sup> M. J. Harris, S. T. Bramwell, D. F. McMorrow, T. Zeiske, and K. W. Godfrey, *Phys. Rev. Lett.* **79**, 2554 (1997).
- <sup>11</sup> S. T. Bramwell and M. J. P. Gingras, *Science* **294**, 1495 (2001).
- <sup>12</sup> N. Shannon, O. Sikora, F. Pollmann, K. Penc, and P. Fulde, *Phys. Rev. Lett.* **108**, 067204 (2012).
- <sup>13</sup> T. Fennell, P. P. Deen, A. R. Wildes, K. Schmalzl, D. Prabhakaran, A. T. Boothroyd, R. J. Aldus, D. F. McMorrow, S. T. Bramwell, *Science* **326**, 415 (2009).
- <sup>14</sup> L. Savary and L. Balents, *Phys. Rev. Lett.* **108**, 037202 (2012).
- <sup>15</sup> K. A. Ross, L. Savary, B. D. Gaulin and L. Balents, *Phys. Rev. X* **1**, 021002 (2011).
- <sup>16</sup> L.-J. Chang, S. Onoda, Y. Su, Y.-J. Kao, K.-D. Tsuei, Y. Yasui, K. Kakurai, and M. R. Lees, *Nature Communications* **3**, 992 (2012).
- <sup>17</sup> H. D. Zhou, C. R. Wiebe, J. A. Janik, L. Balicas, Y. J. Yo, Y. Qiu, J. R. D. Copley, and J. S. Gardner, *Phys. Rev. Lett.* **101**, 227204 (2008).
- <sup>18</sup> S. Onoda and Y. Tanaka, *Phys. Rev. Lett.* **105**, 047201 (2010).
- <sup>19</sup> Y. Chapuis, A. Yaouanc, P. Dalmas de Réotier, C. Marin, S. Vanishri, S. H. Curnoe, C. Văju, and A. Forget, *Phys. Rev. B* **82**, 100402(R) (2010).
- <sup>20</sup> A. Yaouanc, P. Dalmas de Réotier, Y. Chapuis, C. Marin, S. Vanishri, D. Aoki, B. Fåk, L.-P. Regnault, C. Buisson, A. Amato, C. Baines, and A. D. Hillier, *Phys. Rev. B* **84**, 184403 (2011).
- <sup>21</sup> B. D. Gaulin, J. S. Gardner, P. A. McClarty and M. J. P. Gingras, *Phys. Rev. B* **84**, 140402(R) (2011).
- <sup>22</sup> H. Takatsu, H. Kadowaki, T. J. Sato, J. W. Lynn, Y. Tabata, T. Yamazaki, and K. Matsuhira, *J. Phys. Condens. Matter* **24**, 052201 (2011).
- <sup>23</sup> H. R. Molavian and M. J. P. Gingras, *J. Phys.: Condens. Matter* **21**, 172201 (2009).
- <sup>24</sup> K. Matsuhira, Z. Hiroi, T. Tayama, S. Takagi, and T. Sakakibara, *J. Phys. Condens. Matter* **14**, L559 (2002).
- <sup>25</sup> R. Moessner and S. L. Sondhi, *Phys. Rev. B* **68**, 064411 (2003).
- <sup>26</sup> Y. Tabata, H. Kadowaki, K. Matsuhira, Z. Hiroi, N. Aso, E. Ressouche, and B. Fåk, *Phys. Rev. Lett.* **97**, 257205 (2006).
- <sup>27</sup> T. Fennell, S. T. Bramwell, D. F. McMorrow, P. Manuel, and A. R. Wildes, *Nature Physics* **3**, 566 (2007).
- <sup>28</sup> E. Lhotel, C. Paulsen, P. Dalmas de Réotier, A. Yaouanc, C. Marin, and S. Vanishri, *Phys. Rev. B* **86**, 020410(R) (2012).
- <sup>29</sup> S. Legl, C. Krey, S. R. Dunsiger, H. A. Dabkowska, J. A. Rodriguez, G. M. Luke, and C. Pfeiderer, *Phys. Rev. Lett.* **109**, 047201 (2012).
- <sup>30</sup> L. Yin, J. S. Xia, Y. Takano, N. S. Sullivan, Q. J. Li, and X. F. Sun, arXiv:1206.5541.
- <sup>31</sup> Y. Yasui, M. Kanada, M. Ito, H. Harashina, M. Sato, H. Okumura, and K. Kakurai, *J. Phys. Chem. Solids* **62**, 343 (2001).
- <sup>32</sup> K. C. Rule, J. P. C. Ruff, B. D. Gaulin, S. R. Dunsiger, J. S. Gardner, J. P. Clancy, M. J. Lewis, H. A. Dabkowska, I. Mirebeau, P. Manuel, Y. Qiu, and J. R. D. Copley, *Phys. Rev. Lett.* **96**, 177201 (2006).
- <sup>33</sup> H. Cao, A. Gukasov, I. Mirebeau, P. Bonville, and G. Dhalle, *Phys. Rev. Lett.* **101**, 196402 (2008).
- <sup>34</sup> J. P. C. Ruff, B. D. Gaulin, K. C. Rule, and J. S. Gardner, *Phys. Rev. B* **82**, 100401(R) (2010).
- <sup>35</sup> A. P. Sazonov, A. Gukasov, I. Mirebeau, H. Cao, P. Bonville, B. Grenier, and G. Dhalle, *Phys. Rev. B* **82**, 174406 (2010).
- <sup>36</sup> I. Mirebeau, I. N. Goncharenko, P. Cadavez-Peres, S. T. Bramwell, M. J. P. Gingras, and J. S. Gardner, *Nature* **420**, 54 (2002).
- <sup>37</sup> J. P. C. Ruff, B. D. Gaulin, J. P. Castellan, K. C. Rule, J. P. Clancy, J. Rodriguez, and H. A. Dabkowska, *Phys. Rev. Lett.* **99**, 237202 (2007).
- <sup>38</sup> J. P. C. Ruff, Z. Islam, J. P. Clancy, K. A. Ross, H. Nojiri, Y. H. Matsuda, H. A. Dabkowska, A. D. Dabkowski, and B. D. Gaulin, *Phys. Rev. Lett.* **105**, 077203 (2010).
- <sup>39</sup> K. C. Rule and P. Bonville, *J. Phys.: Conf. Ser.* **145**, 012027 (2009).
- <sup>40</sup> S. J. Blundell, *Contemp. Phys.* **40**, 175 (1999).
- <sup>41</sup> N. Hamaguchi, T. Matsushita, N. Wada, Y. Yasui, and M. Sato, *Phys. Rev. B* **69**, 132413 (2004).
- <sup>42</sup> P. J. Baker, J. S. Lord and D. Prabhakaran, *J. Phys.: Condens. Matter* **23**, 306001 (2011).
- <sup>43</sup> We have also performed transverse field  $\mu$ SR and find no evidence of level crossings, although our results are consistent with previous investigations, see Refs. 20,46.
- <sup>44</sup> P. Dalmas de Réotier, A. Yaouanc, L. Keller, A. Cervellino, B. Roessli, C. Baines, A. Forget, C. Văju, P. C. M. Gubbens, A. Amato, and P. J. C. King, *Phys. Rev. Lett.* **96**, 127202 (2006).
- <sup>45</sup> A. Yaouanc and P. Dalmas de Réotier, *Muon Spin Rotation, Relaxation, and Resonance* (Oxford University Press, 2011).
- <sup>46</sup> S. R. Dunsiger, Ph.D. thesis, University of British Columbia, 2000.
- <sup>47</sup> A. Keren, J. S. Gardner, G. Ehlers, A. Fukaya, E. Segal, and Y. J. Uemura, *Phys. Rev. Lett.* **92**, 107204 (2004).
- <sup>48</sup> O. Ofer, A. Keren, and C. Baines, *J. Phys.: Condens. Matter* **19**, 145270 (2007).
- <sup>49</sup> C. P. Slichter, *Principles of Magnetic Resonance* (3<sup>rd</sup> edi-

tion, Springer-Verlag, New York, 1996).